DALTON
FULL PAPER

Synthesis, structure and mechanism of formation of chalcogen-stabilised mixed-metal clusters featuring acetylide bridging and acetylide coupling

Pradeep Mathur,*[a] Moawia O. Ahmed,[a] John H. Kaldis[b] and Michael J. McGlinchey*[b]

[a] *Chemistry Department, Indian Institute of Technology, Powai, Bombay 400 076, India. E-mail: mathur@chem.iitb.ac.in*
[b] *Department of Chemistry, McMaster University, Hamilton, Ontario, Canada L8S 4M1*

Received 6th August 2001, Accepted 8th November 2001
First published as an Advance Article on the web 18th January 2002

Mild thermolysis of a toluene solution of $[(\eta^5\text{-}C_5H_5)Mo(CO)_3(C{\equiv}CPh)]$ and $[Fe_3(CO)_9(\mu_3\text{-}E)_2]$ (E = S, Se) resulted in the formation of mixed-metal clusters, $[(\eta^5\text{-}C_5H_5)_2Mo_2Fe_3(CO)_8(\mu_3\text{-}E)_2\{\mu_5\text{-}CC(Ph)CC(Ph)\}]$ (E = S, **1**; Se, **2**), $[(\eta^5\text{-}C_5H_5)_2Mo_2Fe_4(CO)_9(\mu_3\text{-}E)_2(\mu_4\text{-}CCPh)_2]$ (E = S, **3**; Se, **4**) and $[(\eta^5\text{-}C_5H_5)_2Mo_2Fe_3(CO)_7(\mu_3\text{-}E)_2\{\mu_5\text{-}CC(Ph)C(Ph)C\}]$ (E = S **5**; E = Se **6**) which feature head-to-tail coupling of two acetylide groups, two acetylide groups which remain uncoupled and a tail-to-tail coupling of two acetylide groups, respectively, on the chalcogen-bridged Fe/Mo cluster framework. Under similar conditions, the reaction of $[(\eta^5\text{-}C_5H_5)W(CO)_3(C{\equiv}CPh)]$ and $[Fe_3(CO)_9(\mu_3\text{-}E)_2]$ formed the clusters $[(\eta^5\text{-}C_5H_5)_2W_2Fe_3(CO)_7(\mu_3\text{-}E)_2(\mu_3\text{-}\eta^2\text{-}CCPh)(\mu_3\text{-}\eta^1\text{-}CCH_2Ph)]$ (E = S, **7** or Se, **8**) and $[(\eta^5\text{-}C_5H_5)WFe_2(CO)_8(\mu\text{-}CCPh)]$ (**9**). All compounds have been characterised by IR and ^1H and ^{13}C NMR spectroscopy. The Se-bridged compounds have been further characterised by ^{77}Se NMR spectroscopy. The crystal structures of **1**, **3** and **5**–**9** were elucidated by X-ray diffraction methods.

Introduction

Mononuclear acetylide complexes are versatile building blocks in cluster growth reactions and numerous types of mixed-metal clusters have been prepared by this route.[1–5] This approach has been particularly fruitful for the formation of clusters containing multisite-bound polycarbon units resulting from coupling of acetylide units. Although head-to-head and head-to-tail coupling of acetylides are the usual forms observed, recently, an unusual tail-to-tail coupling has also been reported.[6] Coupling has been observed to take place with, or without, incorporation of a carbonyl group. In our previous reports, we have described the synthesis and structures of clusters obtained by using chalcogen-bridged iron carbonyl clusters with mononuclear acetylide compounds.[7] Our interest in this area stems from previous work on the use of chalcogen bridges in cluster synthesis-reactions, and the large variation in reactivity observed when different chalcogen bridges are used.[8–11] While some variation in the reactivity of the mononuclear acetylide complexes $[(\eta^5\text{-}C_5R_5)M(CO)_3(C{\equiv}CPh)]$ (where R = H or Me and M = Mo or W) with $[Fe_3(CO)_9(\mu_3\text{-}E)_2]$ (where E = S, Se or Te) is expected, we find that the reaction conditions used play a significant role in influencing these reactions. We have previously reported two different types of reaction of $[Fe_3(CO)_9(\mu_3\text{-}E)_2]$ with mononuclear acetylide complexes: those carried out under anaerobic conditions[9,10] and the ones under aerobic conditions.[12,13] In the former case, we have isolated the mixed-metal clusters $[M_2Fe_3(\eta^5\text{-}C_5R_5)_2(CO)_6(\mu_3\text{-}E)_2\{\mu\text{-}CC(Ph)C(Ph)C\}]$ and $[M_2Fe_2(\eta^5\text{-}C_5R_5)_2(CO)_4(\mu_3\text{-}E)_2\{\mu\text{-}CC(Ph)(CO)C(Ph)C\}]$ (M = Mo or W; R = H or Me; E = S, Se or Te) which feature tail-to-tail coupling of acetylide ligands with and without CO. In contrast, under aerobic reaction conditions we were able to isolate complexes containing both oxo and acetylide ligands in the same molecule, as in $[(\eta^5\text{-}C_5Me_5)W(O)(Se_2)(CCPh)]$ and $[(\eta^5\text{-}C_5H_5)_2Mo_2WFe_2(O)_2(S)_2(CO)_9(CCPh)_2]$.

The reactions of $[Fe_3(CO)_9(\mu_3\text{-}E)_2]$ with $[(\eta^5\text{-}C_5R_5)M(CO)_3(C{\equiv}CPh)]$ may be envisaged to occur by mechanisms (a) in which the first step can be either decarbonylation at the iron centre and addition of the chalcogen-bridged iron carbonyl unit to the carbon–carbon triple bond of the metal acetylide compound, or (b) by loss of one or more carbonyls from the metal acetylide compound and complexation by lone pairs of the triply-bridging chalcogen atoms of the tri-iron cluster. Subsequent steps would involve formation of new metal–metal bonds, acetylide coupling, and rearrangements to give the final products. The nature of acetylide coupling, whether it be head-to-head, head-to-tail or tail-to-tail, would depend upon the relative orientations of the metal acetylide units; this in turn may be controlled by the positions of the bridging chalcogen ligands within each cluster. We shall return to this topic after a discussion of the results.

It is known that, at the temperature of refluxing toluene, $[(\eta^5\text{-}C_5H_5)Mo(CO)_3(C{\equiv}CPh)]$ undergoes dimerisation to form $[\{(\eta^5\text{-}C_5H_5)Mo(CO)_2\}\{\mu\text{-}1,2\text{-}PhC{\equiv}CC{\equiv}CPh\}]$ and $[\{(\eta^5\text{-}C_5H_5)Mo(CO)_2\}\{\mu\text{-}1,2\text{-}PhC{\equiv}C(CO)C{\equiv}CPh\}]$, while the tungsten compound, $[(\eta^5\text{-}C_5H_5)W\text{-}(CO)_3(C{\equiv}CPh)]$ decomposes under similar conditions.[7,14] Therefore, to prevent such side reactions of the metal acetylide compounds, we chose to use milder reaction conditions with the goal of obtaining chalcogen-bridged mixed-metal clusters bearing acetylide bridges. The motivation for this work is our continuing interest in new acetylide coupling reactions on chalcogen-stabilised mixed-metal clusters, and our wish to gain a better understanding of the factors influencing the various types of acetylide-coupling on metal clusters.

Results and discussion

Reaction of $[(\eta^5\text{-}C_5H_5)Mo(CO)_3(C{\equiv}CPh)]$ and $[Fe_3(CO)_9(\mu_3\text{-}E)_2]$ (E = S, Se)

When a toluene solution containing $[(\eta^5\text{-}C_5H_5)Mo(CO)_3(C{\equiv}CPh)]$ and $[Fe_3(CO)_9(\mu_3\text{-}E)_2]$ (E = S, Se) was heated at 90 °C for 3 h, under a nitrogen atmosphere, the following new acetylide-coupled mixed-metal clusters were obtained: $[(\eta^5\text{-}C_5H_5)_2Mo_2Fe_3(CO)_8(\mu_3\text{-}E)_2\{\mu_5\text{-}CC(Ph)CC(Ph)\}]$ (E = S, **1** or Se,

DOI: 10.1039/b107090h

Table 1 Spectroscopic data for compounds **1**–**9**

Compound	IR [ν(CO)/cm^{-1}]	^{1}H NMR (δ, $CDCl_3$)	^{13}C NMR (δ, $CDCl_3$)	^{77}Se NMR (δ, $CDCl_3$)
$[(\eta^5\text{-}C_5H_5)_2Mo_2Fe_3(CO)_8(\mu_3\text{-}S)_2\{\mu_5\text{-}CC(Ph)CC(Ph)\}]$ **1**	2062(s), 2025(vs), 1970 (s), 1874(w,brd), 1790(w)	7.26–8.02 (m, C_6H_5), 5.25 (s, C_5H_5), 4.92 (s, C_5H_5)	92.3 (s, C_5H_5), 93.5 (s, C_5H_5), 89.6 (s, C*C*(Ph)CC(Ph)), 88.2 (s, CC(Ph)C*C*(Ph)], 161.2 (s, C*C*(Ph)*C*C(Ph)), 128.6–131.1 (C_6H_5)	
$[(\eta^5\text{-}C_5H_5)_2Mo_2Fe_3(CO)_8(\mu_3\text{-}Se)_2\{\mu_5\text{-}CC(Ph)CC(Ph)\}]$ **2**	2056(s), 2022(vs), 1968 (s), 1870(w,brd), 1787(w)	7.2–8.05 (m, C_6H_5), 5.16 (s, C_5H_5), 4.83 (s, C_5H_5)	91.4 (s, C_5H_5), 93.3 (s, C_5H_5), 89.2 (s, C*C*(Ph)CC(Ph)), 88.8 (s, CC(Ph)C*C*(Ph)], 162.3 (s, C*C*(Ph)*C*C(Ph)), 127.9–130.4 (C_6H_5)	681, 1059
$[(\eta^5\text{-}C_5H_5)_2Mo_2Fe_4(CO)_9(\mu_3\text{-}S)_2(\mu_4\text{-}CCPh)_2]$ **3**	2050(vs), 2000(vs)	7.1–8.77 (m, C_6H_5), 5.56 (s, C_5H_5), 5.46 (s, C_5H_5)	94.2 (s, C_5H_5), 95.3 (s, C_5H_5), 104.0 (s, C*C*Ph)$_2$, 164.3 (s, *C*CPh)$_2$, 127.6–129.4 (C_6H_5)	
$[(\eta^5\text{-}C_5H_5)_2Mo_2Fe_4(CO)_9(\mu_3\text{-}Se)_2(\mu_4\text{-}CCPh)_2]$ **4**	2047(s), 1998(vs)	7.1–8.76 (m, C_6H_5), 5.56 (s, C_5H_5), 5.45 (s, C_5H_5)	91.8 (s, C_5H_5), 92.9 (s, C_5H_5), 104.6 (s, C*C*Ph)$_2$, 165.6 (s, *C*CPh)$_2$, 127.6–129.4 (C_6H_5)	937, 678
$[(\eta^5\text{-}C_5H_5)_2Mo_2Fe_3(CO)_7(\mu_3\text{-}S)_2\{\mu_5\text{-}CC(Ph)C(Ph)C\}]$ **5**	2037(vs), 2017(vs), 1967 (vs)	7.1–7.5 (m, C_6H_5), 5.17 (s, C_5H_5), 5.42 (s, C_5H_5)	93.1 (s, C_5H_5), 91.8 (s, C_5H_5), 127–132 (C_6H_5), 136.2 (s, C_4Ph_2), 142.3 (s, C_4Ph_2), 209.1, 212.1, 217.2, (*C*O).	
$[(\eta^5\text{-}C_5H_5)_2Mo_2Fe_3(CO)_7(\mu_3\text{-}Se)_2\{\mu_5\text{-}CC(Ph)C(Ph)C\}]$ **6**	2033(s), 2013(vs), 1965 (vs)	7.2–7.59 (m, C_6H_5), 5.17 (s, C_5H_5), 5.42 (s, C_5H_5)	94.3 (s, C_5H_5), 92.7 (s, C_5H_5), 128–131 (C_6H_5), 138.4 (s, C_4Ph_2), 140.7 (s, C_4Ph_2), 208.1, 211.0, 216.6 (*C*O).	979, 739
$[(\eta^5\text{-}C_5H_5)_2W_2Fe_3(CO)_7(\mu_3\text{-}S)_2(\mu_3\text{-}\eta^2\text{-}CCPh)(\mu_3\text{-}\eta^1\text{-}CCH_2Ph)]$ **7**	2034(s), 2010(vs), 1960 (vs)	7.2–7.66 (m, C_6H_5), 5.42 (s, C_5H_5), 5.45 (s, C_5H_5), 4.71, 4.77 (d, CH_2), 5.74, 5.81 (d, CH_2)	90.4 (s, C_5H_5), 88.4 (s, C_5H_5), 101.4 (s, *C*CPh), 166.1 (s, *C*CPh), 106.1 (s, *C*CH$_2$Ph), 127.6–129.4 (C_6H_5), 207.8, 209.2, 214.2 (*C*O)	
$[(\eta^5\text{-}C_5H_5)_2W_2Fe_3(CO)_7(\mu_3\text{-}Se)_2(\mu_3\text{-}\eta^2\text{-}CCPh)(\mu_3\text{-}\eta^1\text{-}CCH_2Ph)]$ **8**	2032(s), 2010(vs), 1958 (vs)	7.2–7.7 (m, C_6H_5), 5.42 (s, C_5H_5), 5.45 (s, C_5H_5), 4.67, 4.73 (d, CH_2), 5.75, 5.81 (d, CH_2)	91.0 (s, C_5H_5), 89.7 (s, C_5H_5), 103.6 (s, *C*CPh), 165.4 (s, *C*CPh), 106.7 (s, *C*CH$_2$Ph), 127.6–129.4 (C_6H_5), 206.1, 211.3, 215.6 (*C*O)	657, 730
$[(\eta^5\text{-}C_5H_5)_2WFe_2(CO)_8(\mu\text{-}CCPh)]$ **9**	2065(s), 2034(vs), 2011(s), 1989(vs) 1977(m), 1963(s)	7.6–7.3 (m, C_6H_5), 5.63 (s, C_5H_5)	89.0 (s, C_5H_5), 98.0 (s, *C*CPh), 129.1–132.3 (C_6H_5), 165.0 (s, *CC*Ph); 213.2, 208.3 (*C*O)	

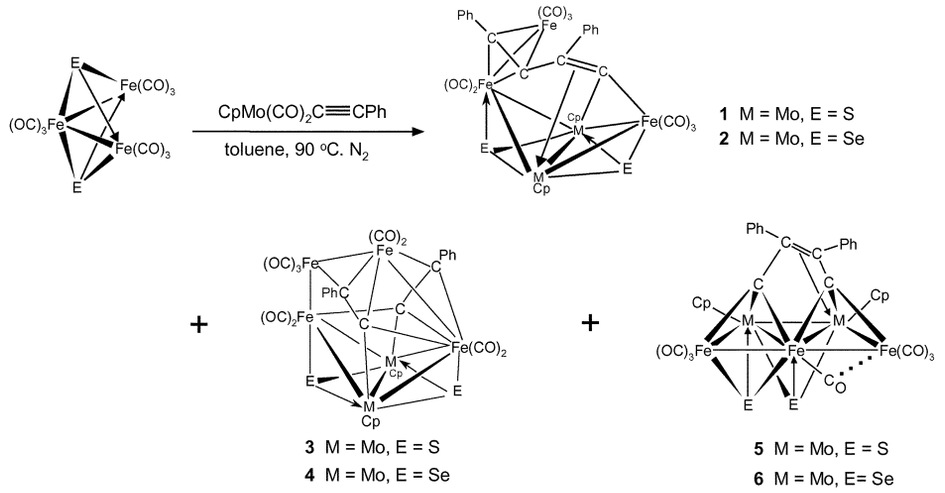

Scheme 1

2), $[(\eta^5\text{-}C_5H_5)_2Mo_2Fe_4(CO)_9(\mu_3\text{-}E)_2(\mu_4\text{-}CCPh)_2]$ (E = S, **3** or Se, **4**) and $[(\eta^5\text{-}C_5H_5)_2Mo_2Fe_3(CO)_7(\mu_3\text{-}E)_2\{\mu_5\text{-}CC(Ph)C(Ph)C\}]$ (**5**: E = S; **6**: E = Se) (Scheme 1, Table 1). The new clusters are stable in the solid state but gradually decompose in solution over a period of hours at room temperature. The solid state structures of **1**, **3**, **5** and **6** were established by single crystal X-ray diffraction studies. Identification of **2** and **4** was made by comparison of their spectroscopic features with those of **1** and **3**, respectively.

The infrared spectra of compounds **1** and **2** show an identical CO stretching pattern in the range 1787–2062 cm^{-1} indicating the presence of bridging as well as terminal carbonyl groups. The ^1H NMR spectra display two signals for the two non-equivalent Cp groups and multiple peaks assignable to the phenyl ring. The ^{77}Se NMR spectrum of **2** shows two signals, indicating non-equivalence of the two Se ligands.

Dark red crystals of **1** were grown by slow evaporation of a hexane–dichloromethane solution and a single crystal X-ray analysis was carried out. Its molecular structure, shown in Fig. 1, consists of a Mo_2Fe_2 butterfly skeleton. The Mo atoms occupy the hinge-sites, Fe atoms are located at the wing-tips and each face of the butterfly is capped by a μ_3-S atom. One wing-tip iron atom is attached to an $Fe(CO)_3$ group. While Fe(1) and Fe(3) each bear three terminal CO groups, Fe(2) has one terminal CO ligand and a second carbonyl group bridged to Fe(3). The Mo–Mo bond distance of 2.6867(5) Å in **1** is slightly longer than the Mo–Mo bond distance of 2.624(2) Å observed in $[(CH_3C_5H_4)_2Mo_2Fe_2(\mu_3\text{-}S)_4(CO)_6]$, which has a planar arrangement of four metal atoms, but shorter than the Mo–Mo bond distances in other clusters which feature a Mo_2Fe_2 butterfly core structure: 2.821(1) Å in $[Cp'Mo_2Fe_2(\mu_3\text{-}S)_2(\mu_3\text{-}CO)_2]$, and 2.846(5) Å in $[Cp_2Mo_2Fe_2(\mu_3\text{-}S)_2(CO)_6(\mu\text{-}CO)_2]$.[15] It is only marginally shorter than the Mo–Mo bond distances of 2.7194(12) Å observed in $[Cp_2Mo_2Fe_2(CO)_6(\mu_3\text{-}S)(\mu_3\text{-}Se)(\mu_4\text{-}Se)]$,[16] and 2.725(2) Å in $[Cp_2Mo_2Fe_2(\mu_3\text{-}S)_2(CO)_6(\mu_4\text{-}Te)]$,[11] in which one and both Mo_2Fe planes respectively are capped by μ_3-S atoms. The average Fe–Mo bond distance of 2.8164 Å in **1** is shorter than the Fe–Mo bond distance of 2.905 Å in $[H(Cp)MoCoFe(CO)_8(\mu_3\text{-}GeBu^t)]$,[17] but close to the average Fe–Mo bond distances of 2.835 Å in $[Cp_2Mo_2Fe_2(\mu_3\text{-}Se)(CO)_7]$ and 2.847 Å in $[Cp_2Mo_2Fe_2(CO)_6(\mu_3\text{-}Se)_2(\mu_4\text{-}Se)]$.[18]

The most significant structural feature of **1** is the head-to-tail acetylide-coupled μ_5-{CC(Ph)CC(Ph)} unit, which acts as an eight electron donor to the cluster core. The C–C bond distances in the C_4 fragment in **1** [C(1)–C(2) = 1.400(4), C(2)–C(9) = 1.467(5) and C(9)–C(10) = 1.351(5) Å], are slightly longer than the C–C bond distances of 1.332(7), 1.366(7), and 1.321(7) Å observed in the C_4 fragment of the head-to-head coupled complex $[Ru_4(CO)_8(PPh_2)_2\{C(Bu^t)CCC(Bu^t)\}]$,[5] but closer to the C–C bond distances of 1.48(4), 1.44(5) and 1.36(5) Å observed in the C_4 fragment of the head-to-tail coupled compound $[Mo_2Os_3(\eta^5\text{-}C_5H_5)_2(CO)_{11}\{CC(Ph)CC(Ph)\}]$.[2]

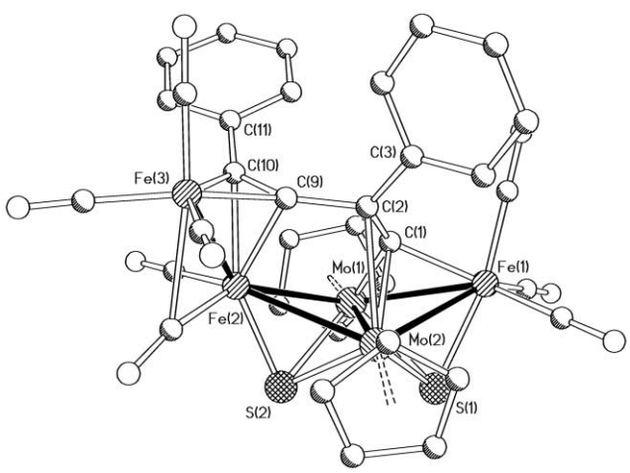

Fig. 1 Molecular structure of $[(\eta^5\text{-}C_5H_5)_2Mo_2Fe_3(CO)_8(\mu_3\text{-}S)_2\{\mu_5\text{-}CC(Ph)CC(Ph)\}]$, **1**. Selected bond lengths [Å] and angles [°]: Mo(1)–C(1) 2.029(3), Mo(1)–S(2) 2.3721(9), Mo(1)–S(1) 2.3806(10), Mo(1)–Mo(2) 2.6867(5), Mo(2)–Fe(1) 2.8025(5), Mo(2)–Fe(2) 2.8774(6), Fe(1)–C(1) 2.027(3), Fe(1)–S(1) 2.2410(10), Mo(1)–Fe(1) 2.7614(6), Fe(2)–S(2) 2.1653(11), Fe(2)–Fe(3) 2.5856(7), C(1)–C(2) 1.400(4), C(2)–C(3) 1.504(5), Mo(1)–Fe(2) 2.8246(6), Mo(2)–C(1) 2.166(3), Mo(2)–S(2) 2.3888(10), Mo(2)–S(1) 2.4064(10), Mo(2)–C(2) 2.490(3); Fe(1)–S(1)–Mo(1) 73.31(3), C(1)–Mo(2)–C(2) 34.12(11), Fe(1)–S(1)–Mo(2) 74.08(3), Mo(1)–S(1)–Mo(2) 68.28(3), Fe(2)–S(2)–Mo(1) 76.85(3), Fe(2)–S(2)–Mo(2) 78.20(3), Mo(1)–S(2)–Mo(2) 68.71(3).

The IR spectra of **3** and **4** display identical carbonyl stretching patterns indicating the presence of only terminally bonded carbonyl groups. Their ^1H and ^{13}C NMR spectra indicate the presence of non-equivalent Cp ligands, and the ^{77}Se NMR spectrum of **4** shows two peaks indicating the presence of two different selenium environments. Black crystals of compound **3** were grown from a hexane–dichloromethane solvent mixture at −5 °C, and its structure was elucidated by a single crystal X-ray diffraction study. The molecular structure of **3** is depicted in Fig. 2; the basic cluster geometry consists of a Mo_2Fe_2 butterfly core whereby the Mo atoms occupy the hinge-sites and two iron atoms, Fe(1) and Fe(4), are located at the wing-tips. The two Mo_2Fe faces are each capped by a μ_3-S atom, and each Mo atom bears an $(\eta^5\text{-}C_5H_5)$ group. The Fe(4) atom at one wing-tip is attached to both Fe(2) and Fe(3), while Fe(1) at the other wing-tip is attached to only one other iron atom, [Fe(2)]. Among the four iron atoms Fe(3) has three terminal carbonyl groups, while Fe(1), Fe(2) and Fe(4) bear only two terminal carbonyl groups each.

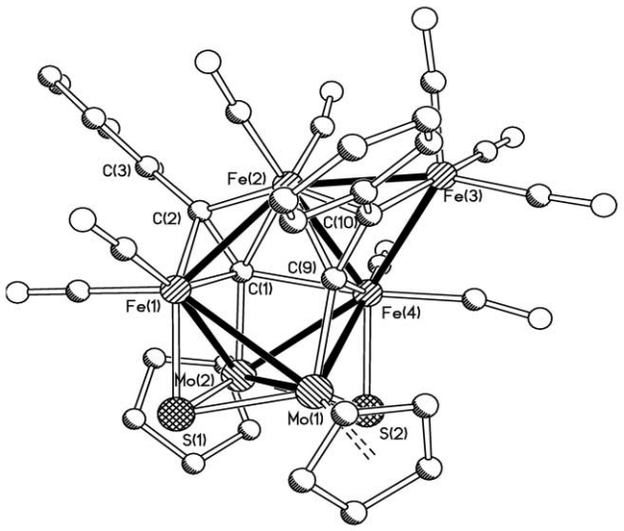

Fig. 2 Molecular structure of $[(\eta^5\text{-}C_5H_5)_2Mo_2Fe_4(CO)_9(\mu_3\text{-}S)_2(\mu_4\text{-}CCPh)_2]$, **3**. Selected bond lengths [Å] and angles [°]: Mo(1)–Fe(4) 2.7453(5), Mo(1)–Mo(2) 2.8416(4), Mo(1)–Fe(1) 2.9574(6), Mo(2)–Fe(1) 2.7214(6), Mo(2)–Fe(4) 2.7763(5), Fe(1)–Fe(2) 2.6487(7), Fe(2)–Fe(3) 2.5296(6), Fe(2)–Fe(4) 2.6008(7), Fe(3)–Fe(4) 2.7418(7), C(1)–C(2) 1.362(4), C(2)–C(3) 1.481(4), C(9)–C(10) 1.391(4); Fe(1)–S(1)–Mo(1) 80.68(3), Fe(1)–S(1)–Mo(2) 72.25(3), Mo(1)–S(1)–Mo(2) 74.61(3), Fe(4)–S(2)–Mo(2) 75.18(3), Fe(4)–S(2)–Mo(1) 73.67(3), Mo(2)–S(2)–Mo(1) 74.99(3), C(2)–C(1)–Mo(2) 146.8(3), C(2)–C(1)–Fe(1) 73.2(2), C(10)–Fe(2)–C(1) 119.75(12), Fe(4)–C(1)–Fe(2) 70.78(9), C(1)–C(2)–C(3) 137.4(3), C(1)–C(2)–Fe(2) 84.4(2), Fe(2)–C(2)–Fe(1) 81.79(12), C(10)–C(9)–Mo(1) 150.0(2).

The terminal carbon atom, C(1) of one of the two phenylacetylene groups acts as μ_4 bridging (three Fe's and one Mo) [Fe(1)–C(1) = 2.028(3) Å, Fe(2)–C(1) = 2.264(3) Å, Fe(4)–C(1) = 2.221(3) Å and Mo(2)–C(1) = 1.995(3) Å]. The other terminal carbon atom, C(9), is μ_3 bridging (two Fe's and one Mo), while each of the two inner carbon atoms is bonded to two Fe atoms as well as bearing a phenyl group. The Mo–Mo bond distance of 2.8416(4) Å in **3** is longer than the Mo–Mo bond distance in **1** [2.6867(5) Å] but comparable with the Mo–Mo bond distance of 2.846(4) Å in $[Cp_2Mo_2Fe_2(\mu_3\text{-}S)_2(CO)_6(\mu\text{-}CO)_2]$.[15] The average Mo–Fe bond distance of 2.8026 Å in **3** is similar to the average Mo–Fe bond distances of 2.8164 Å in **1**. It is shorter than the average Mo–Fe bond distance of 2.902 Å in $[Cp_2Mo_2Fe_2(CO)_6(\mu_4\text{-}Te)(\mu_3\text{-}Se)_2]$.[16] The average Mo–C bond distance of 2.0145 Å in **3** is also very close to the average Mo–C bond distances of 2.0975 Å in **1**. Spectroscopic features indicate that compound **4** is isostructural with **3**.

The IR spectra of **5** and **6** display identical carbonyl stretching patterns in the range 1965 to 2036 cm^{-1}, indicating the presence of only terminally bonded carbonyls. The ^1H NMR spectra of **5** and **6** each show two signals revealing the presence of two non-equivalent Cp ligands, as well as a multiplet for the phenyl group protons. The ^{77}Se NMR spectrum of **6** exhibits two peaks for the two types of selenium atom in the molecule. Dark brown crystals of **5** and **6** were grown from a hexane–dichloromethane solvent mixture at −5 °C, and an X-ray diffraction study was undertaken. As shown in Figs. 3 and 4, respectively, clusters **5** and **6** are isostructural. The basic cluster geometry can be described as consisting of a twisted bow-tie type Fe_3MoE unit, one face of which is capped by the second Mo atom, and the second face is capped by one terminal carbon atom of an {(CC(Ph)C(Ph)C} unit. Each molybdenum atom is bonded to an $(\eta^5\text{-}C_5H_5)$ ligand. Among the three iron centres, Fe(2) has one terminal carbonyl group, while both Fe(1) and Fe(3) atoms each bear three terminal CO groups. The second E atom in the molecule acts as μ_3 bridging and caps the triangle formed by two Mo atoms and the middle Fe atom of the bow-tie. An unusual feature of these molecules is the {(CC(Ph)-C(Ph)C} unit, in which one terminal carbon atom, C(9), triply

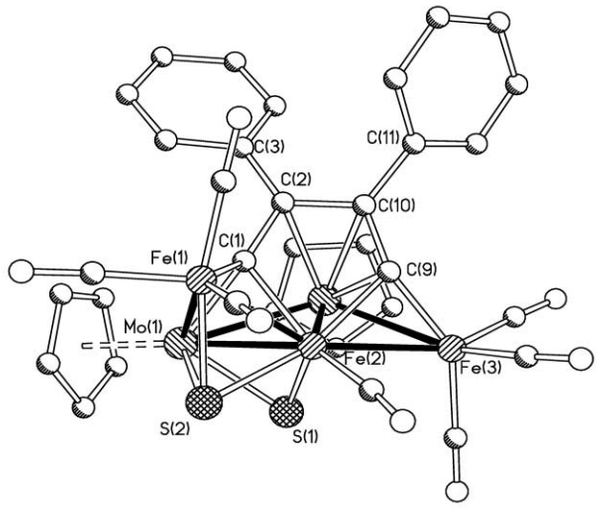

Fig. 3 Molecular structure of $[(\eta^5\text{-}C_5H_5)_2Mo_2Fe_3(CO)_7(\mu_3\text{-}S)_2\{\mu_5\text{-}CC(Ph)C(Ph)C\}]$, **5**. Selected bond lengths [Å] and angles [°]: Mo(1)–Fe(2) 2.3623(13), Mo(1)–Fe(1) 2.371(4), Mo(1)–Mo(2) 2.9683(4), Mo(2)–Fe(2) 2.5535(7), Mo(2)–Fe(3) 2.8605(8), Fe(1)–Fe(2) 2.5713(9), Fe(2)–Fe(3) 2.5942(9), 2.5942(9), Fe(2)–C(9) 2.006(4), Fe(2)–C(1) 2.075(4), C(1)–C(2) 1.447(6), C(2)–C(10) 1.456(5), C(9)–C(10) 1.407(6); Fe(2)–Mo(1)–Fe(1) 57.48(2), Fe(2)–Mo(1)–Mo(2) 54.42(2), Fe(1)–Mo(1)–Mo(2) 96.90(2), Fe(2)–Mo(2)–Fe(3) 56.92(2), Mo(2)–Fe(2)–Fe(1) 114.04(3), Mo(1)–Fe(2)–Fe(1) 65.45(2), Mo(2)–Fe(2)–Fe(3) 67.51(2), Mo(1)–Fe(2)–Fe(3) 135.45(3), Fe(1)–Fe(2)–Fe(3) 148.78(3), C(2)–C(1)–Mo(1) 141.9(3), C(1)–C(2)–C(10) 110.7(4), C(1)–C(2)–C(3) 122.5(4), C(10)–C(2)–C(3) 126.5(4), C(1)–C(2)–Mo(2) 73.8(2), C(10)–C(2)–Mo(2) 74.4(2), C(9)–C(10)–C(2) 112.5(4), C(9)–C(10)–Mo(2) 65.2(3).

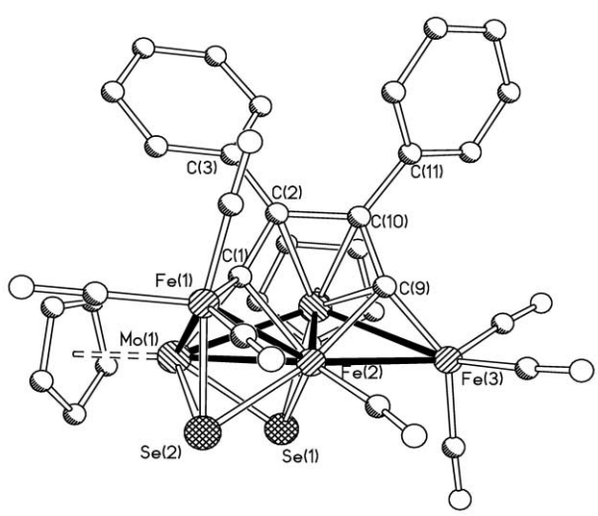

Fig. 4 Molecular structure of $[(\eta^5\text{-}C_5H_5)_2Mo_2Fe_3(CO)_7(\mu_3\text{-}Se)_2\{\mu_5\text{-}CC(Ph)C(Ph)C\}]$, **6**. Selected bond lengths [Å] and angles [°]: Mo(1)–Fe(2) 2.5811(14), Mo(1)–Fe(1) 2.7996(14), Mo(1)–Mo(2) 2.9844(4), Mo(2)–Fe(2) 2.5724(14), Mo(2)–Fe(3) 2.860(2), Fe(1)–Fe(2) 2.571(2), Fe(2)–Fe(3) 2.603(2), Fe(3)–C(9) 1.837(9), C(1)–C(2) 1.467(10), C(2)–C(10) 1.445(10), C(2)–C(3) 1.472(10), C(9)–C(10) 1.424(10), C(10)–C(11) 1.509(9); Fe(1)–Fe(2)–Fe(3) 149.08(5), Fe(2)–Se(1)–Mo(2) 63.98(4), Mo(2)–Se(1)–Mo(1) 73.40(4), Fe(1)–Se(2)–Fe(2) 65.49(5), Fe(1)–Se(2)–Mo(1) 71.03(4), Fe(2)–Mo(1)–Fe(1) 56.92(4), Fe(2)–Mo(1)–Mo(2) 54.48(3), Fe(1)–Mo(1)–Mo(2) 96.65(4), Fe(1)–Fe(2)–Mo(2) 114.33(6), Fe(1)–Fe(2)–Mo(1) 65.82(4), Mo(2)–Fe(2)–Mo(1) 70.78(4), Mo(2)–Fe(2)–Fe(3) 67.09(5), Mo(1)–Fe(2)–Fe(3) 134.76(6), Fe(2)–Fe(3)–Mo(2) 55.94(4), C(10)–C(2)–C(1) 110.7(7), C(10)–C(2)–C(3) 127.7(6), C(1)–C(2)–C(3) 121.0(7), C(10)–C(2)–Mo(2) 74.1(4), C(9)–C(10)–C(2) 111.5(6).

bridges one face of the Fe_3MoE bow-tie: Fe(2), Fe(3) and Mo(2), and the other terminal carbon atom, C(1), triply bridges the face described by Fe(1), Fe(2) and Mo(1) centres. The inner carbon atoms, C(2) and C(9), that bear the phenyl groups chelate the closer molybdenum atom, Mo(2).

The Mo–Mo bond distance of 2.9844(4) Å in **6** is slightly longer than the Mo–Mo bond distance of 2.9683(4) Å in **5**, and both are longer than the Mo–Mo bond distances in **1** and **3** [2.6867(5) and 2.8416(4) Å, respectively], but shorter than the Mo–Mo bond distance of 3.096(1) Å, in the Se-bridged compound, $[Cp_2Mo_2Fe(\mu_3\text{-}Se)_2(CO)_7]$.[19] All the C–C bond distances in the C_4 ligand in **5** and **6** are almost equal [1.447(6), 1.456(5), 1.407(6) Å and 1.467(10), 1.445(10), 1.424(10) Å respectively]; these distances are comparable with C–C bond lengths [1.421(6), 1.428(5), 1.439(5) Å] in the C_4 fragment of the previously reported tail-to-tail coupled product $[(\eta^5\text{-}C_5Me_5)_2W_2Fe_3(CO)_6(\mu_3\text{-}S)_2\{\mu_4\text{-}CC(Ph)C(Ph)C\}]$.[6] In clusters **5** and **6**, both molybdenum atoms and also Fe(1) can be assigned 18 electrons if it is assumed that one chalcogen atom contributes two electrons to Fe(2); formally Fe(2) and Fe(3) would then possess 19 and 17 electrons, respectively, but this situation is alleviated since the single carbonyl on Fe(2) is weakly semi-bridged to Fe(3).

Reaction of $[(\eta^5\text{-}C_5H_5)W(CO)_3(C{\equiv}CPh)]$ and $[Fe_3(CO)_9(\mu_3\text{-}E)_2]$ (E = S, Se)

On thermolysis of a toluene solution of $[(\eta^5\text{-}C_5H_5)W(CO)_3(C{\equiv}CPh)]$ and $[Fe_3(CO)_9(\mu_3\text{-}E)_2]$ (E = S, Se or Te) at 90 °C, under a nitrogen atmosphere, for 3 hours, the following three compounds were isolated: $[(\eta^5\text{-}C_5H_5)_2W_2Fe_3(CO)_7(\mu_3\text{-}E)_2(\mu_3\text{-}\eta^2\text{-}CCPh)(\mu_3\text{-}\eta^1\text{-}CCH_2Ph)]$ (**7**: E = S; **8**: E = Se) and $[(\eta^5\text{-}C_5H_5)WFe_2(CO)_8(CCPh)]$ (**9**) (Scheme 2, Table 1). Reaction with the Te-bridged starting compound, $[Fe_3(CO)_9(\mu_3\text{-}Te)_2]$ led to substantial decomposition and only trace amounts of the starting materials were isolated after 3 hours.

The infrared spectra of **7** and **8** display identical CO stretching patterns indicating the presence of only terminally bonded carbonyl groups. There is a shift of the corresponding carbonyl stretching bands to lower frequencies for the selenium-bridged compound, **8**, as compared to its sulfur-bridged analogue, **7**. The ^{1}H NMR spectra of **7** and **8** each show two signals attributable to the presence of two non-equivalent Cp ligands, as well as a multiplet for the phenyl ring. Two sets of doublets for both compounds are seen for the non-equivalent (diastereotopic) protons of the CH_2 group. The ^{77}Se NMR spectrum of **8** shows two signals at δ 657.1 and 729.7, indicating the presence of two types of Se ligand. Dark brown crystals of **7** and **8** were grown from a hexane–dichloromethane solvent mixture at −4 °C, and single crystal X-ray diffraction experiments were carried out. As depicted in Figs. 5 and 6, respectively, clusters **7** and **8** are isostructural. The basic cluster geometry can be described as consisting of a FeW_2E tetrahedron (E = S or Se). A second chalcogen atom, E, bridges the W–W bond and also forms a bond to the iron atom of an $Fe(CO)_3$ unit which bridges one of the W–Fe edges of the basic tetrahedron. This $Fe(CO)_3$ unit is also bonded to a CCH_2Ph unit which in turn also bridges the same Fe–W tetrahedron edge. The CCH_2Ph group thus functions as a carbyne group capping a Fe_2W face. The second Fe–W edge of the tetrahedron also has a bridging $Fe(CO)_3$ unit, thus forming another Fe_2W face which has a $\mu_3\text{-}\eta^2$-CCPh group above it. These compounds feature a $(\mu_3\text{-}\eta^1\text{-}CCH_2Ph)$ group, in which the terminal carbon atom triply bridges two Fe and one W atoms, while the inner carbon atom attached to the phenyl group has apparently abstracted two hydrogen atoms. Suspecting that these two extra hydrogen atoms might have been derived from the toluene solvent, perhaps *via* radical intermediates, the reaction was repeated in deuterated toluene. The product is spectroscopically identical except that the ^{1}H NMR resonances for methylene protons are now absent, confirming the solvent as the origin of the CH_2 group.

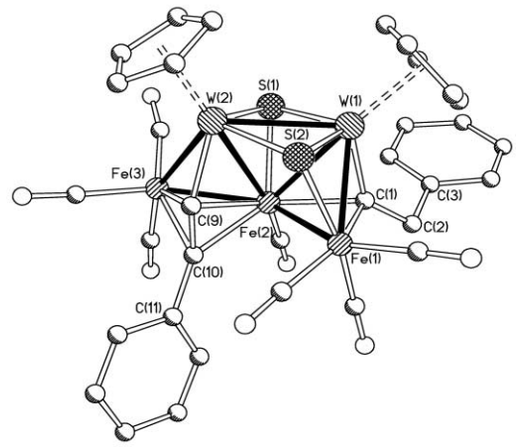

Fig. 5 Molecular structure of $[(\eta^5\text{-}C_5H_5)_2W_2Fe_3(CO)_7(\mu_3\text{-}S)_2(\mu_3\text{-}\eta^2\text{-}CCPh)(\mu_3\text{-}\eta^1\text{-}CCH_2Ph)]$, **7**. Selected bond lengths [Å] and angles [°]: W(1)–Fe(2) 2.6726(12), W(1)–Fe(1) 2.7131(11), W(1)–W(2) 2.8259(5), W(2)–Fe(2) 2.6577(13), W(2)–Fe(3′) 2.76(2), W(2)–Fe(3) 2.95(3), Fe(1)–Fe(2) 2.601(2), Fe(2)–Fe(3) 2.51(3), C(1)–C(2) 1.535(12), C(2)–C(3) 1.523(13), C(9)–C(10) 1.330(12); C(10)–C(11) 123.6(6), Fe(3)–Fe(2)–Fe(1) 139.7(5), C(2)–C(1)–Fe(1) 123.6(6), C(3)–C(2)–C(1) 116.1(8), C(10)–C(9)–Fe(2) 71.0(5), W(2)–C(9)–Fe(2) 83.5(3).

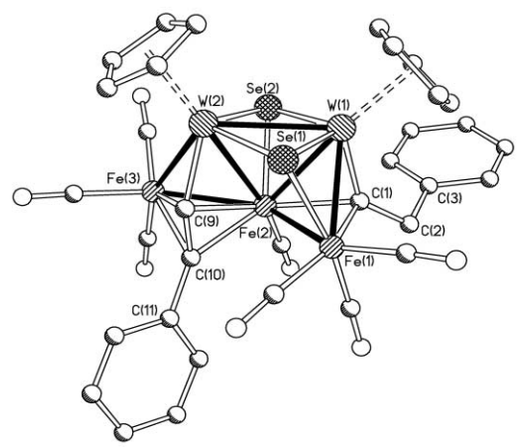

Fig. 6 Molecular structure of $[(\eta^5\text{-}C_5H_5)_2W_2Fe_3(CO)_7(\mu_3\text{-}Se)_2(\mu_3\text{-}\eta^2\text{-}CCPh)(\mu_3\text{-}\eta^1\text{-}CCH_2Ph)]$, **8**. Selected bond lengths [Å] and angles [°]: W(1)–Fe(2) 2.6972(11), Fe(1)–Fe(2) 2.6075(15), W(1)–Fe(1) 2.7443(10), W(1)–W(2) 2.8747(4), W(2)–Fe(2) 2.6831(12), W(2)–Fe(3) 2.8397(14), Fe(2)–Fe(3) 2.5761(15), C(1)–C(2) 1.548(11), C(2)–C(3) 1.514(11), C(9)–C(10) 1.331(11), C(10)–C(11) 1.470(10); Fe(3)–Fe(2)–Fe(1) 137.11(6), C(2)–C(1)–Fe(1) 122.3(5), C(3)–C(2)–C(1) 116.9(7), C(9)–C(10)–C(11) 139.3(8), C(9)–C(10)–Fe(2) 72.0(4), C(11)–C(10)–Fe(2) 143.4(6), C(9)–C(10)–Fe(3) 68.5(4), C(11)–C(10)–Fe(3) 125.8(6).

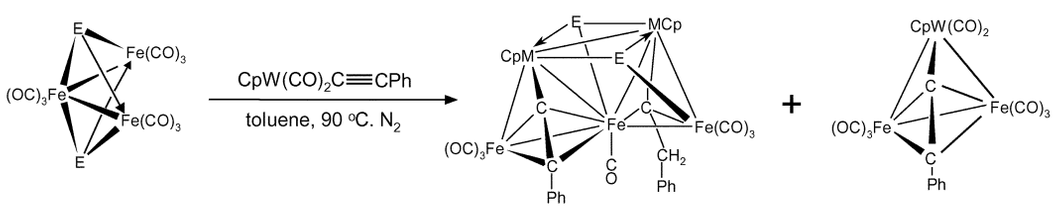

7 M = W, E = S
8 M = W, E = Se

9

Scheme 2

The W–W distance of 2.8259(5) Å in **7** is shorter than the W–W distance of 2.8747(4) Å in **8**, but is closer to the W–W distance of 2.8277(4) Å observed in $[(\eta^5\text{-}C_5H_5)_2W_2Fe_2(CO)_4(\mu_3\text{-}E)_2\{\mu\text{-}CC(Ph)COC(Ph)C\}]$.[7] In compound **8**, the average W–Fe bond distance of 2.7855 Å is slightly longer than the average W–Fe bond distance of 2.7484 Å in **7**. These distances are shorter than the W–Fe bond distances of 2.802(4) and 2.829(4) Å in $[Fe_2W(CO)_{10}(Se)_2]$.[10] In both compounds, the C–C bond distance of 1.331(11) Å in the CCPh fragment, indicating olefinic bond order, is shorter than the C–C bond distance of 1.470(11) Å in the CCH_2Ph fragment.

The infrared spectrum of **9** reveals the presence of only terminally bonded carbonyl groups. The ^1H and ^{13}C NMR spectra show one signal for the $\eta^5\text{-}C_5H_5$ ligand, and multiplets for the phenyl group protons. The ^{13}C NMR spectrum also shows two signals for the coordinated CCPh group in the region expected for coordinated C≡C atoms, and for the terminal carbonyl carbon atoms. Red crystals of **9** were obtained from a hexane–dichloromethane mixture by slow evaporation of the solvents at −5 °C, and its molecular structure, established by single crystal X-ray methods, is shown in Fig. 7. This molecule

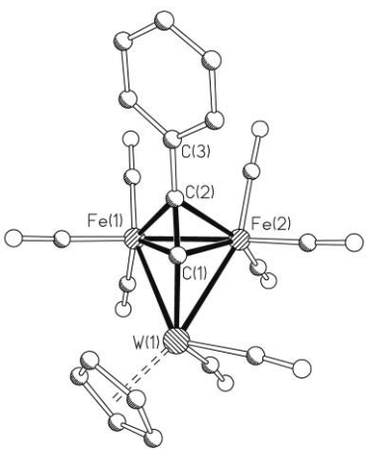

Fig. 7 Molecular structure of $[(\eta^5\text{-}C_5H_5)WFe_2(CO)_8(CCPh)]$, **9**. Selected bond lengths [Å] and angles [°]: W(1)–Fe(1) 2.8362(7), W(1)–Fe(2) 2.8993(8), W(1)–C(1) 1.996(5), Fe(1)–Fe(2) 2.4908(12), Fe(1)–C(1) 2.042(5), Fe(2)–C(1) 2.046(5), Fe(2)–C(2) 2.161(6), C(1)–C(2) 1.294(7); C(1)–Fe(1)–W(1) 44.72(15), C(2)–Fe(2)–Fe(1) 51.45(14), Fe(1)–Fe(2)–W(1) 62.96(2), W(1)–C(1)–Fe(1) 89.2(2), W(1)–C(1)–Fe(2) 91.7(2), Fe(1)–C(1)–Fe(2) 75.1(2), C(1)–W(1)–Fe(2) 44.87(15), C(1)–W(1)–Fe(1) 46.05(14), C(2)–Fe(1)–W(1) 81.50(14).

has a triangular Fe_2W core structure, in which the tungsten atom is associated with an $(\eta^5\text{-}C_5H_5)$ group and two CO ligands; the CCPh moiety is σ-bonded to the W atom but also forms a transverse bridge over the Fe–Fe bond. Each Fe atom has three terminally bonded carbonyl groups. The asymmetric unit of the crystal structure comprises two molecules and, although their bond distances are closely similar, they are markedly different in the torsion angles relating to peripheral groups. In **9**, the WFe_2 triangle is nearly isosceles with the bond distances W(1)–Fe(1) = 2.8362(7) Å, W(1)–Fe(2) = 2.8993(8) Å and Fe(1)–Fe(2) = 2.4908(12) Å. Overall, the geometry of **9** is very similar to the previously reported and related compounds $[CpWFe_2(CO)_8CC(Tol)]$,[20] and $[CpWRu_2(CO)_8(CCPh)]$.[21] The W(1)–C(1) bond distance of 1.996(5) Å in **9** is similar to the corresponding bond distance of 1.999(15) Å in $[CpWFe_2(CO)_8CC(Tol)]$, and 1.976(8) Å in $[CpWRu_2(CO)_8(CCPh)]$. The C(1)–C(2) bond distance of 1.294(7) Å in **9** is longer than the average C–C distance of acetylene molecules (1.20 Å),[22] but close to the C–C bond distance of 1.30(2) Å observed in $[CpWFe_2(CO)_8CC(Tol)]$.

Mechanistic considerations

The isolation of a number of subtly different products from a series of closely related reactions is suggestive of a system in which an initially common mechanistic pathway diverges at various points, and leads to apparently disparate, but actually fundamentally similar, products. We here advance a mechanistic scenario which, starting from a common intermediate, readily accounts for *all* the observed products. While we fully recognize the speculative nature of such proposals, we feel that it is incumbent upon us to try to rationalise this fascinating chemistry.

We suggest that the initially formed cluster, **10**, is one in which the capping S (or Se) groups of $Fe_3(CO)_9(\mu_3\text{-}E)_2$ each coordinate to a $CpM(CO)_2C{\equiv}CPh$ unit, analogous to the previously known reaction of $Os_3(CO)_9S_2$ and $W(CO)_6$ which yields $Os_3(CO)_9(\mu_3\text{-}S)[(\mu_3\text{-}S)W(CO)_5]$.[23] The process can now continue from **10** in one of two ways: (a) cleavage of *each* S (or Se) bond to a *terminal* iron $Fe(CO)_3$ unit to give **11**, or (b) cleavage of *both* bonds from the capping atom to the *central* $Fe(CO)_3$ moiety to produce **12** (see Scheme 5).

In the first case, as depicted in Scheme 3, elimination of three carbonyls and formation of four molybdenum (or tungsten) to iron bonds can give rise to **13** and **14**, successively, whereby the chalcogens cap Fe_2M triangular faces. Now, if *both* S (or Se) atoms migrate onto M_2Fe faces they remain *trans* to each other and place the alkynyl units on opposite sides of the cluster, as in **15**. Subsequent loss of a CO ligand from the central iron yields an Fe_2C_2 tetrahedron. Addition of the second alkyne across the other Fe–Fe bond is accompanied by migration of an S (or Se) from the central to a terminal iron, thus generating a carbene-type intermediate **16**. As previously discussed, abstraction of two hydrogens from the solvent leads to the observed product, **7** or **8**. Note that, in this particular case, the *double* migration of either S or Se from the Fe_2M to M_2Fe faces occurs only when M = W, and is presumably controlled by the strength of the tungsten–chalcogen bond.

If we return to intermediate **14** in Scheme 3, but allow *only one* sulfur or selenium to migrate onto an adjacent Mo_2Fe face, as in **17**, the alkynes are now on the same side of the cluster; addition of both C≡CPh moieties across Fe–Fe edges gives two carbene sites, in **18**, that can couple to give the tail-to-tail linked products, **5** or **6**, as depicted in Scheme 4.

As stated at the outset, a second scenario begins with cleavage of the bonds between the capping sulfurs (or seleniums) and the *central* iron atom as in **12**. Loss of three carbonyl ligands and formation of four Fe–Mo bonds produces the cluster **19** in which two molybdenums and two irons adopt a butterfly arrangement. Loss of another CO and migration of *both* chalcogens onto the neighbouring M_2Fe faces would lead to the cluster **20** in which both alkynes are poised to add across Fe–Fe vectors. In **21**, one Fe_2C_2 tetrahedron has been formed, and once again the mechanism can branch. If the Fe–Fe bond breaks to give **22**, subsequent cleavage of one molybdenum-alkyne linkage and coupling to the β-carbon of the other alkyne unit leads *via* **23** to the observed head-to-tail linked products **1** and **2**, as illustrated in Scheme 5.

Finally, returning to cluster **21**, loss of two carbonyls and addition of the second alkyne across the remaining iron–iron bond, would lead to the *closo* seven-vertex pentagonal-bipyramidal system **24**, comprised of a Mo_2C_2Fe five-membered ring capped by two $Fe(CO)_2$ moieties (Scheme 6). The required electrons to achieve the 16 skeletal electron count are provided by the triply-bridging chalcogen and phenylcarbynyl units. In fact, this system was not observed in the present case; instead, addition of an $Fe(CO)_3$ fragment brings about cluster expansion to the somewhat distorted triangular dodecahedral eight-vertex *closo* clusters, **3** and **4**.

The cluster framework of **3** is illustrated in Fig. 8 which depicts a $(CpMo)_2[(Fe(CO)_2]_4(C)_2$ triangular dodecahedron capped by triply-bridging chalcogens and carbynes. To achieve the required skeletal electron count of **18**, one of the iron vertices has an extra carbonyl ligand which breaks the intrinsic two-fold symmetry of the cluster.

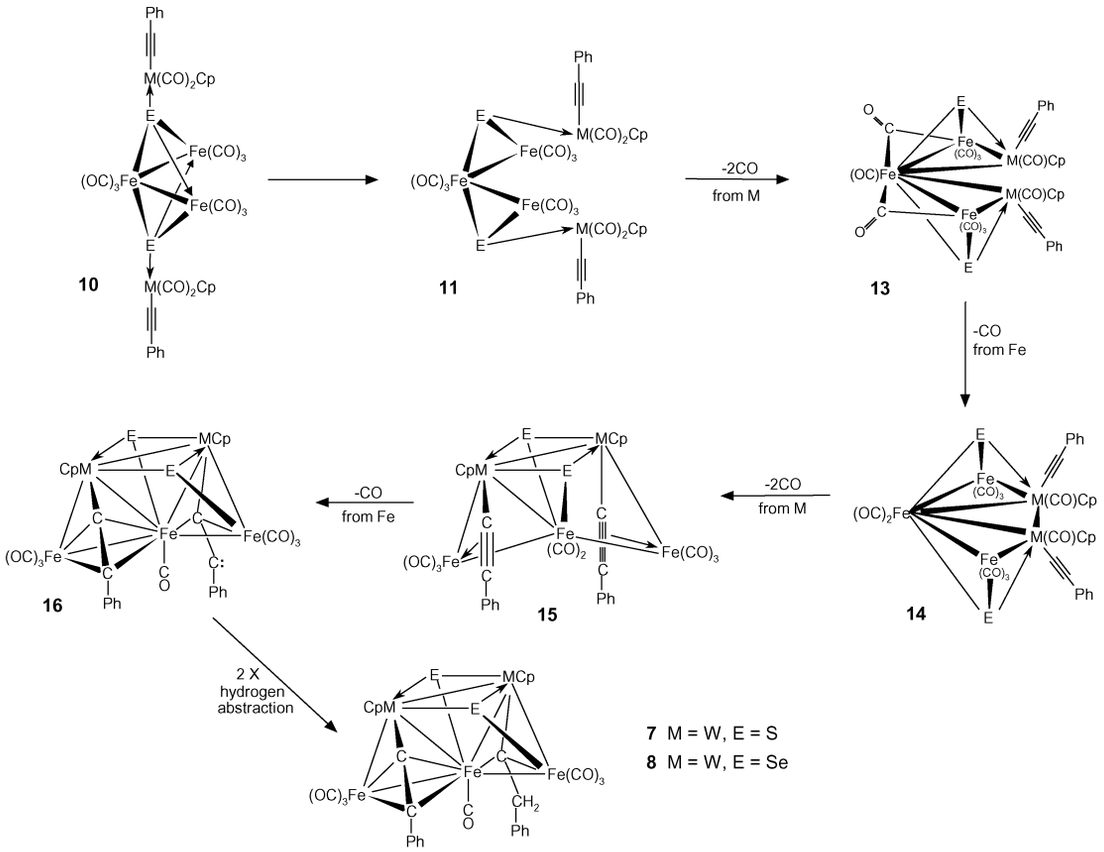

Scheme 3

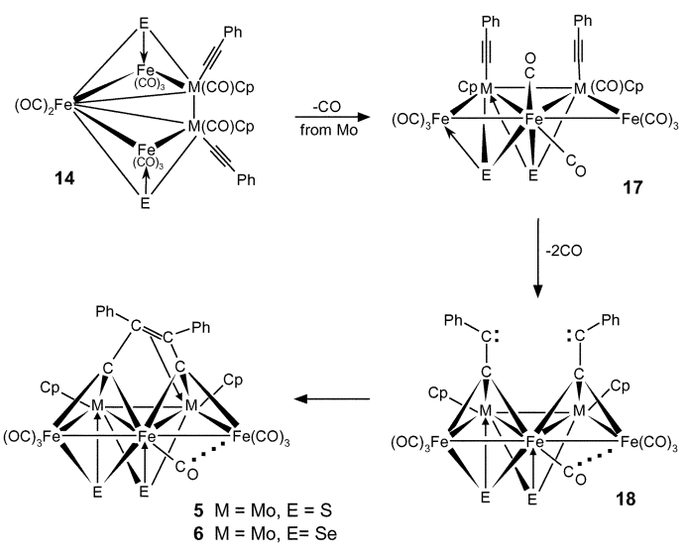

Scheme 4

Finally, we note that the $CpW(CO)_2[Fe(CO)_3]_2(PhCC)$ cluster, **9**, not only has the skeletal electron count appropriate for a *closo* trigonal bipyramid, but also is a motif present in the clusters **7** and **8**. It is evident from Figs. 5 and 6, that the atoms Fe(2), Fe(3), C(9), C(10) and W(2) make up a trigonal bipyramidal unit, and cluster **9** presumably arises from fragmentation during, or subsequent to, the formation of **7** and **8**.

Concluding remarks

The acetylide complexes, $[M(\eta^5\text{-}C_5H_5)(CO)_3(C{\equiv}CPh)]$ (M = Mo or W) react with $[Fe_3(CO)_9(\mu_3\text{-}E)_2]$ (E = S or Se) under mild thermolytic conditions to give a variety of acetylide-bridged mixed-metal clusters. The molybdenum acetylide complex reacts to form three types of clusters: these products feature head-to-tail coupling of two acetylides, as in **1** and **2**, tail-to-tail coupling of the two acetylide groups, as in **5** and **6**, and a third product in which the acetylide groups are not directly coupled, but are bridged head-to-head by an $Fe(CO)_2$ unit, as in **3** and **4**. These products can be envisaged as arising from a common intermediate in which the triply-bridging chalcogen bonds initially to a $Mo(\eta^5\text{-}C_5H_5)(CO)_2(C{\equiv}CPh)$ unit, and subsequently yields isomeric Mo_2Fe_3 clusters. Migration of one, or both, of the S (or Se) atoms such that they cap Mo_2Fe faces now leaves the alkynyl moieties in sites such that different modes of coupling are sterically viable.

In contrast, the tungsten acetylide compound, $(\eta^5\text{-}C_5H_5)\text{-}W(CO)_3(C{\equiv}CPh)$, reacts to yield clusters whereby acetylide coupling has not occurred, but in which both sulfurs (or seleniums) now triply-bridge W_2Fe faces. The W/Fe acetylide-

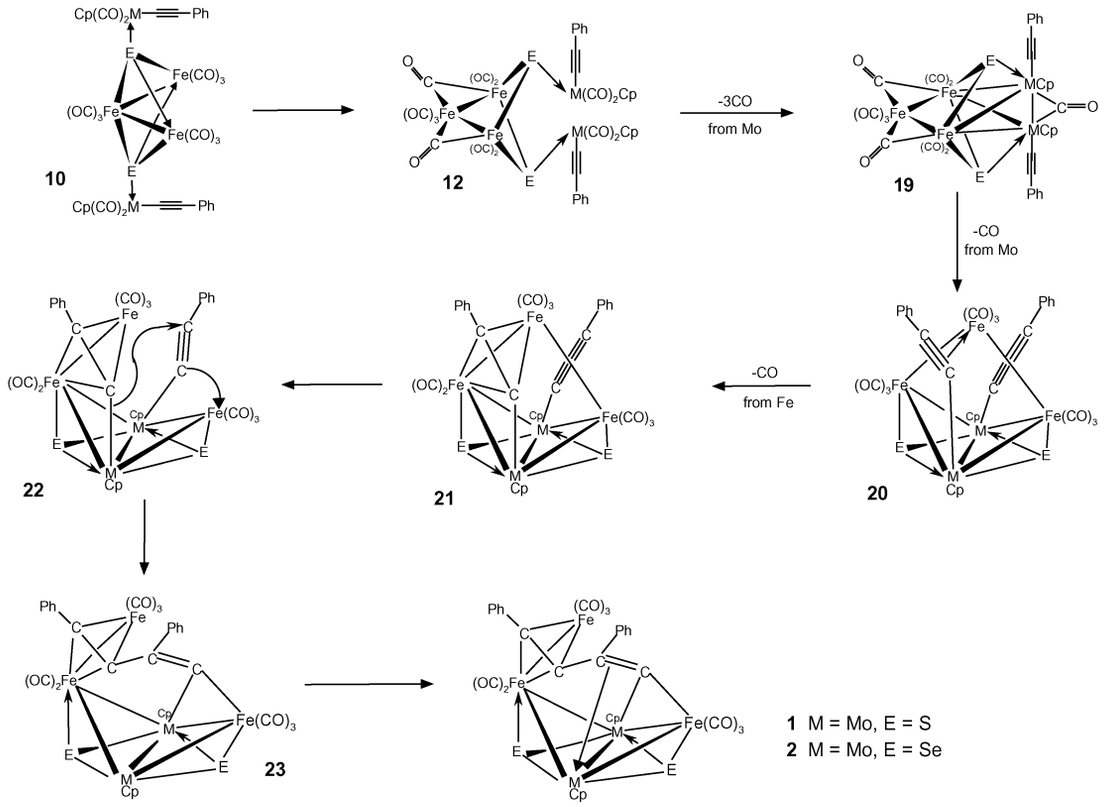

Scheme 5

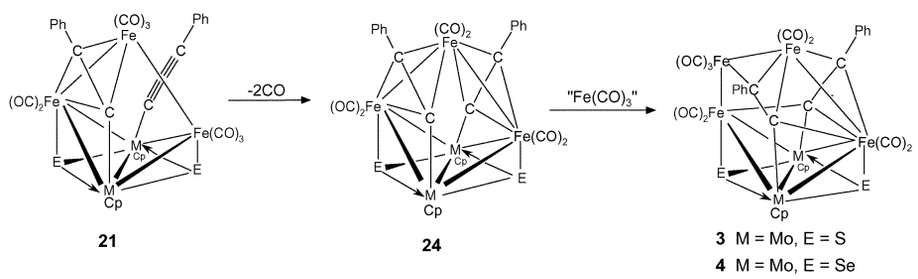

Scheme 6

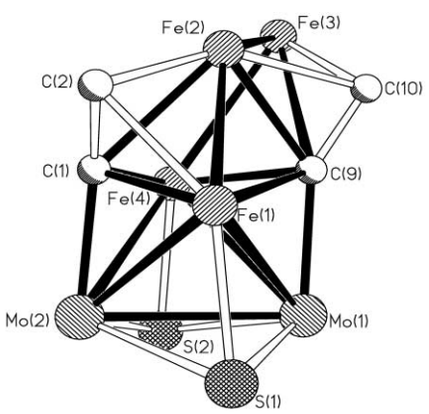

Fig. 8 Skeletal framework of $[(\eta^5\text{-}C_5H_5)_2Mo_2Fe_4(CO)_9(\mu_3\text{-}S)_2(\mu_4\text{-}CCPh)_2]$, **3**.

bridged clusters **7** and **8** also contain a W–W bonded Cp_2W_2 unit as well as an intact Fe_3E_2 unit. The two acetylide moieties remain uncoupled and display different bonding modes; one is attached to an Fe_2W face of the cluster in a μ_3-η^2 mode, and this bonding mode is also seen in the cluster **9**, which is formed in minor yield. The second acetylide group in **7** and **8** caps a second Fe_2W face in a μ_3-η^1 mode. The β-carbon atom of this acetylide group abstracts two H atoms from the solvent and thus a μ_3-CCH_2Ph group is formed. Efforts are in progress to explore photolytic reaction conditions to gain further mechanistic insights into the formation of acetylide-bridged mixed-metal clusters stabilised by chalcogen ligands.

Experimental

1. General procedures

Reactions and manipulations were performed using standard Schlenk techniques under an atmosphere of pre-purified argon. Solvents were purified, dried and distilled under an argon or nitrogen atmosphere prior to use. Infrared spectra were recorded on a Nicolet Impact 400 FT spectrometer as dichloromethane solutions in 0.1 mm path length cells, and NMR (^{13}C and ^{77}Se) spectra on a Varian VXR-300S spectrometer in $CDCl_3$. The ^{77}Se NMR measurements were made at an operating frequency of 57.23 MHz using 90° pulses with 1.0 s delay and 1.0 s acquisition time and referenced to Me_2Se (δ 0). Elemental analyses were performed on a Carlo-Erba automatic analyser. The compounds $[Fe_3(CO)_9(\mu_3\text{-}E)_2]$ (E = S, Se)[24] and $[(\eta^5\text{-}C_5H_5)M(CO)_3\{C{\equiv}C(Ph)\}]$, (M = W or Mo)[25] were prepared by established procedures. Conditions used for preparation of **1**–**9**, and yields of products are summarized in Table 2.

Table 2 Experimental conditions used for the preparation of **1–9**

Compound	Reactants/mg (mmol)	Yield/mg (%)	Analysis (%): Calc. (found)	Mp/°C[a]
$[(\eta^5\text{-}C_5H_5)_2Mo_2Fe_3(CO)_8(\mu_3\text{-}S)_2\{\mu_5\text{-}CC(Ph)CC(Ph)\}]$ **1**	$[Fe_3(CO)_9(\mu_3\text{-}S)_2]$ + $[Cp_2Mo(CO)_3(CC(Ph)]$ 134 (0.28) 150 (0.433)	14 (20)	C, 41.67 (41.56) H, 2.06 (2.16)	210–211
$[(\eta^5\text{-}C_5H_5)_2Mo_2Fe_3(CO)_8(\mu_3\text{-}Se)_2\{\mu_5\text{-}CC(Ph)CC(Ph)\}]$ **2**	$[Fe_3(CO)_9(\mu_3\text{-}Se)_2]$ + $[Cp_2Mo(CO)_3(CC(Ph)]$ 126 (0.28) 150 (0.433)	11 (15)	C, 38.03 (37.9) H, 1.88 (2.0)	206–208
$[(\eta^5\text{-}C_5H_5)_2Mo_2Fe_4(CO)_9(\mu_3\text{-}S)_2(\mu_4\text{-}CCPh)_2]$ **3**	$[Fe_3(CO)_9(\mu_3\text{-}S)_2]$ + $[Cp_2Mo(CO)_3(CC(Ph)]$ 134 (0.28) 150 (0.433)	23 (30)	C, 39.51 (39.3) H, 1.89 (2.2)	223–225
$[(\eta^5\text{-}C_5H_5)_2Mo_2Fe_4(CO)_9(\mu_3\text{-}Se)_2(\mu_4\text{-}CCPh)_2]$ **4**	$[Fe_3(CO)_9(\mu_3\text{-}Se)_2]$ + $[Cp_2Mo(CO)_3(CC(Ph)]$ 126 (0.28) 150 (0.433)	17 (20)	C, 36.31 (35.91) H, 1.74 (1.99)	219–221
$[(\eta^5\text{-}C_5H_5)_2Mo_2Fe_3(CO)_7(\mu_3\text{-}S)_2\{\mu_5\text{-}CC(Ph)C(Ph)C\}]$ **5**	$[Cp_2Mo(CO)_3(CC(Ph)]$ + $[Fe_3(CO)_9(\mu_3\text{-}S)_2]$ 150 (0.433) 134(0.28)	31 (30)	C, 41.63 (42.03) H, 2.12 (2.35)	200–202
$[(\eta^5\text{-}C_5H_5)_2Mo_2Fe_3(CO)_7(\mu_3\text{-}Se)_2\{\mu_5\text{-}CC(Ph)C(Ph)C\}]$ **6**	$[Cp_2Mo(CO)_3(CC(Ph)]$ + $[Fe_3(CO)_9(\mu_3\text{-}Se)_2]$ 150 (0.433) 126 (0.28)	29 (26)	C, 37.90 (38.11) H, 1.93 (2.08)	195–197
$[(\eta^5\text{-}C_5H_5)_2W_2Fe_3(CO)_7(\mu_3\text{-}S)_2(\mu_3\text{-}\eta^2\text{-}CCPh)(\mu_3\text{-}\eta^1\text{-}CCH_2Ph)]$ **7**	$[Cp_2W(CO)_3(CC(Ph)]$ + $[Fe_3(CO)_9(\mu_3\text{-}S)_2]$ 200 (0.461) 134 (0.28)	46 (35)	C, 35.08 (34.39) H, 1.96 (2.15)	245–248
$[(\eta^5\text{-}C_5H_5)_2W_2Fe_3(CO)_7(\mu_3\text{-}Se)_2(\mu_3\text{-}\eta^2\text{-}CCPh)(\mu_3\text{-}\eta^1\text{-}CCH_2Ph)]$ **8**	$[Cp_2W(CO)_3(CC(Ph)]$ + $[Fe_3(CO)_9(\mu_3\text{-}Se)_2]$ 200 (0.461) 126 (0.28)	42 (30)	C, 32.31 (32.59) H, 1.81 (1.89)	243–245
$[(\eta^5\text{-}C_5H_5)_2WFe_2(CO)_8(CCPh)]$ **9**	$[Fe_3(CO)_9(\mu_3\text{-}S)_2]$ + $[Cp_2W(CO)_3(CC(Ph)$ 134 (0.28) 200 (0.461)	19 (18)	C, 36.78 (36.57) H, 1.47 (1.66)	188–190

[a] With decomposition.

2. Reaction of $[Fe_3(CO)_9(\mu_3\text{-}E)_2]$ (E = S or Se) with $[(\eta^5\text{-}C_5H_5)\text{-}Mo(CO)_3(C{\equiv}C(Ph)]$

In a typical reaction, a toluene solution (50 mL) containing $[(\eta^5\text{-}C_5H_5)Mo(CO)_3\{CC(Ph)\}]$ (150 mg, 0.433 mmol) and one equivalent of $[Fe_3(CO)_9(\mu_3\text{-}E)_2]$ (E = S or Se) was heated at 90 °C for 3 h. The solution was allowed to cool to room temperature, filtered through Celite to remove insoluble material and the solvent was removed *in vacuo*. The residue was dissolved in dichloromethane and subjected to chromatographic work-up on silica-gel TLC plates. Elution with a CH_2Cl_2–hexane (30/70 v/v) mixture yielded the following, in order of elution: red $[(\eta^5\text{-}C_5H_5)_2Mo_2Fe_3(CO)_8(\mu_3\text{-}E)_2\{\mu_5\text{-}CC(Ph)CC(Ph)\}]$ [E = S (**1**; 14 mg, 20%), or Se (**2**; 11 mg, 15%)], black $[(\eta^5\text{-}C_5H_5)_2Mo_2Fe_4(CO)_9(\mu_3\text{-}E)_2(\mu_4\text{-}CCPh)_2]$ [E = S (**3**; 23 mg, 30%), or Se (**4**; 16.7 mg, 20%)] and dark brown $[(\eta^5\text{-}C_5H_5)_2\text{-}Mo_2Fe_3(CO)_7(\mu_3\text{-}E)_2\{\mu_5\text{-}CC(Ph)C(Ph)C\}]$ [E = S (**5**; 31 mg, 30%), or Se (**6**; 29 mg, 26%)].

3. Reaction of $[Fe_3(CO)_9(\mu_3\text{-}E)_2]$ (E = S or Se) with $[(\eta^5\text{-}C_5H_5)\text{-}W(CO)_3(C{\equiv}C(Ph)]$

In a typical reaction, a toluene solution (50 mL) containing $[(\eta^5\text{-}C_5H_5)W(CO)_3\{C{\equiv}C(Ph)\}]$ (200 mg, 0.461 mmol) and one equivalent of $[Fe_3(CO)_9(\mu_3\text{-}E)_2]$ (E = S or Se) was heated at 90 °C for 3 h, under an atmosphere of nitrogen. The solution was allowed to cool to room temperature, filtered through Celite to remove any insoluble material and the solvent was removed *in vacuo*. The residue was dissolved in dichloromethane and subjected to chromatographic work-up on silica-gel TLC plates. Elution with a CH_2Cl_2–hexane (30/70 v/v) mixture yielded the following, in order of elution: dark brown $[(\eta^5\text{-}C_5H_5)_2W_2Fe_3(CO)_7(\mu_3\text{-}E)_2(\mu_3\text{-}\eta^2\text{-}CCPh)(\mu_3\text{-}\eta^1\text{-}CCH_2Ph)]$ [E = S (**7**; 46 mg, 35%), or Se (**8**; 42 mg, 30%)] and red $[(\eta^5\text{-}C_5H_5)\text{-}WFe_2(CO)_8(CCPh)]$ (**9**, 19 mg, 18%).

X-Ray crystal determinations of 1, 3 and 5–9

X-Ray crystallographic data were collected from single crystal samples of **1** (0.32 × 0.30 × 0.05 mm^3), **3** (0.26 × 0.22 × 0.08 mm^3), **5** (0.22 × 0.16 × 0.12 mm^3), **6** (0.30 × 0.25 × 0.08 mm^3), **7** (0.25 × 0.22 × 0.16 mm^3), **8** (0.30 × 0.22 × 0.06 mm^3) and **9** (0.42 × 0.28 × 0.16 mm^3), mounted on glass fibres. Crystal data and structure refinement details for **1**, **3** and **5**–**9** are listed in Table 3. Data were collected using a P4 Bruker diffractometer, equipped with a Bruker SMART 1K charge coupled device (CCD) area detector, using the program SMART,[26] and a rotating anode, using graphite-monochromated Mo-Kα radiation (λ = 0.71073 Å). The crystal-to-detector distance was 4.987 cm, and the data collection was carried out in 512 × 512 pixel mode, utilising 2 × 2 pixel binning. The initial unit cell parameters were determined by a least-squares fit of the angular settings of the strong reflections, collected by a 12° scan in 40 frames over three different sections of reciprocal space (160 frames in total). A complete sphere of data was collected, to better than 0.8 Å resolution at 298 K. Upon completion of the data collection, the first 50 frames were recollected in order to improve the decay correction analyses. Processing was carried out using the program SAINT,[27] which applied Lorentz and polarisation corrections to the three-dimensionally integrated diffraction spots. The program SADABS,[28] was utilised for the scaling of diffraction data, the application of a decay correction, and an empirical absorption correction based on redundant reflections for all data sets except the twinned compound **5**, for which no absorption correction was applied. The structures were solved by using the direct-methods procedure in the Bruker SHELXL program library,[29] and refined by full-matrix least squares methods on F^2 with anisotropic thermal parameters for all non-hydrogen atoms. Hydrogen atoms were added as fixed contributors at calculated positions, with isotropic thermal parameters based on the carbon atom to which they were bonded.

Table 3 Crystal data and structure refinement for **1**, **3** and **5**–**9**

	1	**3**	**5**	**6**	**7**	**8**	**9**
Empirical formula	$C_{34}H_{20}Fe_3Mo_2O_8S_2$	$C_{35}H_{20}Fe_4Mo_2O_9S_2$	$C_{33}H_{20}Fe_3Mo_2O_7S_2$	$C_{33}H_{20}Fe_3Mo_2O_7S_2$	$C_{33}H_{22}Fe_3O_7S_2W_2$	$C_{33}H_{22}Fe_3O_7Se_2W_2$	$C_{21}H_{10}Fe_2O_8W$
Formula weight	980.05	1063.91	952.04	1045.84	1129.88	1223.68	685.84
Temperature/K	298(2)	299(2)	299(2)	299(2)	298(2)	298(2)	298(2)
Wavelength/Å	0.71073	0.71073	0.71073	0.71073	0.71073	0.71073	0.71073
Crystal system	Monoclinic	Monoclinic	Triclinic	Triclinic	Monoclinic	Monoclinic	Monoclinic
Space group	$P2_1/n$	$C2/c$	$P\bar{1}$	$P\bar{1}$	$P2_1/n$	$P2_1/n$	$P2_1/c$
a/Å	10.2463(9)	16.3700(5)	8.87776(11)	8.871(3)	10.8005(8)	10.7612(2)	8.0835(2)
b/Å	18.9432(9)	15.7216(5)	10.9285(13)	10.901(3)	16.9398(9)	17.0519(3)	14.3002(2)
c/Å	17.4513(4)	28.2246(6)	16.850(2)	17.446(5)	18.5162(12)	18.832(1)	37.4493(3)
α/°	90	90	89.310(2)	92.066(5)	90	90	90
β/°	92.538(5)	99.1690(10)	85.743(2)	98.906(6)	92.877(3)	92.73(1)	92.2130(10)
γ/°	90	90	80.224(2)	105.792(6)	90	90	90
Volume/Å^3	3383.9(3)	7171.1(4)	1588.5(3)	1598.3(8)	3383.4(4)	3451.77(9)	4325.75(13)
Z	4	8	2	2	4	4	8
Calculated density/Mg m^{-3}	1.924	1.971	1.990	2.173	2.218	2.355	2.106
Absorption coefficient/mm^{-1}	2.151	2.424	2.286	4.418	8.199	10.025	6.674
F(000)	1928	4176	936	1008	2136	2280	2608
Crystal size/mm	0.05 × 0.30 × 0.32	0.08 × 0.22 × 0.26	0.12 × 0.16 × 0.22	0.30 × 0.25 × 0.08	0.25 × 0.22 × 0.16	0.30 × .22 × 0.06	0.16 × 0.28 × 0.42
θ range for data collection/°	1.59 to 25.00	1.46 to 25.00	1.21 to 25.00	19 to 25.00	1.63 to 25.00	1.61 to 25.00	1.09 to 25.00
Index ranges	$-12 \le h \le 13$ $-24 \le k \le 24$ $-22 \le l \le 22$	$-20 \le h \le 21$ $-20 \le k \le 19$ $-36 \le l \le 32$	$-10 \le h \le 11$ $-14 \le k \le 14$ $-21 \le l \le 21$	$-11 \le h \le 11$ $-13 \le k \le 14$ $-22 \le l \le 22$	$-14 \le h \le 13$ $-21 \le k \le 21$ $-23 \le l \le 24$	$-12 \le h \le 13$ $-22 \le k \le 21$ $-24 \le l \le 23$	$-10 \le h \le 9$ $-16 \le k \le 18$ $-47 \le l \le 48$
Reflections collected	25378	26923	15220	12038	25413	26018	32487
Independent reflections	5776 [R(int) = 0.0453]	6329 [R(int) = 0.0498]	15180	5604 [R(int) = 0.0675]	5948 [R(int) = 0.0610]	6084 [R(int) = 0.0733]	7623 [R(int) = 0.0444]
Refinement method	Full-matrix least-squares on F^2	Full-matrix least-squares on F^2	Full-matrix least-squares on F^2	Full-matrix least-squares on F^2	Full-matrix least-squares on F^2	Full-matrix least-squares on F^2	Full-matrix least-squares on F^2
Data/restraints/parameters	5753/0/443	6317/0/470	15180/0/426	5563/0/425	5946/0/437	6065/0/425	7608/0/578
Goodness-of-fit on F^2	0.966	0.947	0.978	0.835	1.097	0.997	1.017
Final R indices [$I > 2\sigma(I)$]	$R1 = 0.0286$, $wR2 = 0.0563$	$R1 = 0.0288$, $wR2 = 0.0463$	$R1 = 0.0473$, $wR2 = 0.1195$	$R1 = 0.0477$, $wR2 = 0.0830$	$R1 = 0.0453$, $wR2 = 0.0694$	$R1 = 0.0370$, $wR2 = 0.0727$	$R1 = 0.0306$, $wR2 = 0.0537$
R indices (all data)	$R1 = 0.0520$, $wR2 = 0.0627$	$R1 = 0.0584$, $wR2 = 0.0514$	$R1 = 0.0681$, $wR2 = 0.1300$	$R1 = 0.1026$, $wR2 = 0.1178$	$R1 = 0.0670$, $wR2 = 0.0729$	$R1 = 0.0638$, $wR2 = 0.0808$	$R1 = 0.0516$, $wR2 = 0.0585$
Extinction coefficient	0.00052(6)	0.000062(7)	0.0014(3)	0.00062(12)	0.00041(2)	0.00026(3)	0.00069(3)
Largest diff. peak and hole/e Å^{-3}	0.388 and −0.381	0.345 and −0.339	0.614 and −0.549	0.892 and −0.994	1.384 and −1.204	1.489 and −1.018	0.673 and −0.509
Max./min. effective transmission	0.719342/0.472290	0.737047/0.593250	1.000000/0.576991	1.000000/0.719161	0.338091/0.240722	0.266840/0.112488	1.000000/0.576991

Compound **5** was a non-merohedral twin, solved using GEMINI,[30] by integrating and indexing the data for each component independently. The data were subsequently combined and flagged, and the calculated intensity contribution of the secondary component was subtracted from the overlapped data, scaled by using its refined fractional contribution. Compound **6** crystallized as a multiple crystal. GEMINI,[30] was used to separate the diffractional contributions of each of the two single crystals comprising the sample examined. The diffraction data from the predominant crystal were used to solve the structure, while the remaining data were discarded since there was very little overlap. Only 41 data were suppressed due to their high F_o/F_c ratio from intensity contributions by the second crystal fragment. The $Fe(CO)_3$ moiety of Fe(3) in compound **7** contained a positional disorder. The two disordered units were restrained with similar thermal parameters and refined to two slightly different positions on the face of the $WFeC_2$ cluster. The relative occupancy of the major component was 0.63(2). Compound **9** crystallised with two crystallographically unrelated molecules in the unit cell.

CCDC reference numbers 168671–168677.

See http://www.rsc.org/suppdata/dt/b1/b107090h/ for crystallographic data in CIF or other electronic format.

Acknowledgements

P. M. thanks the Council of Scientific and Industrial Research (India) for financial support, and the Royal Society of Chemistry for the award of a Journals Grant for International Authors. Financial support from the Natural Sciences and Engineering Research Council of Canada (NSERC) to M. J. M. is gratefully acknowledged. J. H. K. thanks NSERC and the Province of Ontario for graduate fellowships.

References

1 E. Delgado, Y. Chi, W. Wang, G. Hogarth, P. J. Low, G. D. Enright, S.-M. Peng, G.-H. Lee and A. J. Carty, *Organometallics*, 1998, **17**, 2936.
2 C.-H. Wu, Y. Chi, S.-M. Peng and G.-H. Lee, *J. Chem. Soc., Dalton Trans.*, 1990, 3025.
3 P. Blenkiron, G. D. Enright and A. J. Carty, *Chem. Commun.*, 1997, 483.
4 A. J. Carty, G. D. Enright and G. Hogarth, *Chem. Commun.*, 1997, 1883.
5 Y. Chi, A. J. Carty, P. Blenkiron, E. Delgado, G. D. Enright, W. Wang, S.-M. Peng and G.-H. Lee, *Organometallics*, 1996, **15**, 5269.
6 P. Mathur, M. O. Ahmed, A. K. Dash and M. G. Walawalkar, *J. Chem. Soc., Dalton Trans.*, 1999, 1795.
7 P. Mathur, M. O. Ahmed, A. K. Dash, M. G. Walawalkar and V. G. Puranik, *J. Chem. Soc., Dalton Trans.*, 2000, 2916.
8 P. Mathur, B. Manimaran, R. Trivedi, C. V. V. Satyanarayana and R. K. Chadha, *J. Cluster Sci.*, 1998, **9**, 45.
9 P. Mathur, P. Sekar, A. L. Rheingold and L. M. Liable-Sands, *J. Chem. Soc., Dalton Trans.*, 1997, 2949.
10 P. Mathur, P. Sekar, C. V. V. Satyanarayana and M. F. Mahon, *J. Chem. Soc., Dalton Trans.*, 1996, 2173.
11 P. Mathur, M. M. Hossain, S. B. Umbarkar, C. V. V. Satyanarayana, A. L. Rheingold, L. M. Liable-Sands and G. P. A. Yap, *Organometallics*, 1996, **15**, 1898.
12 P. Mathur, S. Mukhopadhyay, M. O. Ahmed, G. K. Lahiri, S. Chakraborty and M. G. Walawalkar, *Organometallics*, 2000, **19**, 5787.
13 P. Mathur, M. O. Ahmed, A. K. Dash and J. H. Kaldis, *Organometallics*, 2000, **19**, 941.
14 N. A. Ustynyuk, V. N. Vinogradova, V. N. Korneva, D. N. Kravtsov, V. G. Andrianov and Y. T. Struchkov, *J. Organomet. Chem.*, 1984, **277**, 285.
15 P. D. Williams, M. D. Curtis and D. N. Duffy, *Organometallics*, 1983, **2**, 165.
16 P. Mathur, S. Ghose, M. M. Hossain, C. V. V. Satyanarayana and M. F. Mahon, *J. Organomet. Chem.*, 1997, **543**, 189.
17 P. Gusbeth and H. Vahrenkamp, *Chem. Ber.*, 1985, **118**, 1770.
18 P. Mathur, M. M. Hossain and A. L. Rheingold, *Organometallics*, 1993, **12**, 2029.
19 P. Mathur, Md. M. Hossain and A. L. Rheingold, *Organometallics*, 1994, **13**, 3909.
20 D.-K. Hawang, Y. Chi, S.-M. Peng and G.-H. Lee, *Organometallics*, 1990, **9**, 2709.
21 M. Green, K. Marsden, I. D. Salter, F. G. A. Stone and P. J. Woodward, *J. Chem. Soc., Chem. Commun.*, 1983, 446.
22 J. March, *Advanced Organic Chemistry*, 3rd edn., Wiley, New York, 1985, ch. 1.
23 R. D. Adams, I. T. Horvàth and S. Wang, *Inorg. Chem.*, 1985, **24**, 1728.
24 P. Mathur, D. Chakrabarty, M. M. Hossain, R. S. Rashid, V. Rugmini and A. L. Rheingold, *Inorg. Chem.*, 1992, **31**, 1106.
25 M. I. Bruce, M. G. Humphrey, J. G. Matisons, S. K. Roy and A. G. Swincer, *Aust. J. Chem.*, 1984, **37**, 1955.
26 SMART, Release 4.05, Bruker AXS Inc., Madison, WI 53711, 1996.
27 SAINT, Release 4.05, Bruker AXS Inc., Madison, WI 53711, 1996.
28 G. M. Sheldrick, SADABS, Göttingen University, Germany, 1996.
29 G. M. Sheldrick, SHELXTL, Version 5.03, Bruker AXS Inc., Madison, WI 53711, 1994.
30 R. Sparks, GEMINI, Autoindexing Program for Twinned Crystals, Version 1.01, Bruker AXS Inc., Madison, WI 53711, 1999.